Reducing fuel cost and enhancing the resource utilization rate in energy economic load dispatch problem

Chao Chen

- Key Laboratory of Complex System Control Theory and Application, Tianjin University of Technology, Tianjin, 300384, China

E-mail: chao_chen@email.tjut.edu.cn

Linan Qu

- State Key Laboratory of Reliability and Intelligence of Electrical Equipment, Hebei University of Technology, Tianjin 300130, China
- China Electric Power Research Institute (Nanjing), Nanjing 210003, China

E-mail: qulinan@epri.sgcc.com.cn

Ming-Lang Tseng *(Corresponding author)

- Institute of Innovation and Circular Economy, Asia University, Taiwan
- Department of Medical Research, China Medical University Hospital, China Medical University, Taichung, Taiwan

E-mail: tsengminglang@gmail.com; tsengminglang@asia.edu.tw

Lingling Li

- State Key Laboratory of Reliability and Intelligence of Electrical Equipment, Hebei University of Technology, Tianjin 300130, China

E-mail: lilinglinglaoshi@126.com; lilingling@hebut.edu.cn

Chih-Cheng Chen

- Department of Business Administration, Mingdao University, Taiwan

E-mail: thomasba@mdu.edu.tw

Ming K. Lim

- Adam Smith Business School, University of Glasgow, United Kingdom

Email: Ming.Lim@glasgow.ac.uk

Reducing fuel cost and enhancing the resource utilization rate in energy economic load dispatch problem

Abstract

This study contributes for solving the economic load dispatch (ELD) problem to reduce the energy waste caused by thermal generation units and promotes cleaner and sustainable production in the power industry. Electricity is produced by thermal power plants; however, thermal power generation involves low economic benefits and high pollution levels, which hinders cleaner and sustainable production in the power industry. An improved manta ray foraging optimization (IMRFO) algorithm is developed for solving the ELD problem and realizing the cleaner and economic goal of the thermal units. The characteristics of the novel method present that: (1) Sine and cosine adaptations were introduced in the manta ray foraging optimization algorithm to enhance its adaptive ability; (2) a nonlinear convergence factor was presented to enhance the convergence speed; and (3) a differential evolution algorithm was introduced in the original algorithm to enhance robustness. Three typical ELD test systems were selected to prove the feasibility of the IMRFO-based solution method. The results indicated that IMRFO algorithm obtained the most competitive scheduling strategy compared with the existing methods. Improving the economy of power system operation is beneficial to realize cleaner and sustainable power production.

Keywords: Resource utilization; manta ray foraging optimization algorithm; economic load dispatch; algorithm improvement; energy conservation

Nomenclature		NPZ_e	The number of prohibited operation areas
F_e	Cost function	$P^L_{e,j}$	The first prohibited operation area
F_c	Total fuel cost	$P^U_{e,j}$	The maximum prohibited operating area
m	The number of generator units	P^l_e	Lower output bounds
P_e	Output power	P^u_e	Upper output bounds
α_e, β_e and γ_e	Fuel cost coefficients	x^d_k	Location of the k_{th} individual
$P_{e,\min}$	Minimum output power	x^d_{best}	Current optimal position
δ_e and ε_e	Cost coefficients	a	Weight coefficient
B_1, B_2 and B_3	Transmission loss coefficients	L	The maximum values of iterations
P_{loss}	System transmission loss	l	The current values of iterations
P_{load}	Load demand	x^d_{rand}	Random location
$P_{e,\min}$	Lower bounds	Ub^d	Upper limit
$P_{e,\max}$	Upper bounds	Lb^d	Lower limit
P_e^0	The output before the change	r_1	Random values between [0, 1]
DR_e	Ramp-down rate	r_2	Random values between [0, 1]
UR_e	Ramp-up rate	C	Cosine adaptation

S	Sine adaptation	w	Nonlinear convergence factor
$w_{\min}$	Lower limit of w	$w_{\max}$	Upper limit of w
$Z^*_{e,t}$	A newly created individual	$Z_{best,t}$	Optimal value at the t_{th} generation
D	Scaling factor	R	Crossover probability
$f(Z^*_{e,t})$	Fitness function	$f(Z_{e,t})$	Fitness function

Reducing fuel cost and enhancing the resource utilization rate in energy economic load dispatch problem

1. Introduction

Energy demand has driven the sustained economic, especially for electricity resource efficiency. Electricity is supplied to consumers from production plants through the power system, although the current situation involves insufficient development of the energy storage equipment (Chen et al., 2019; Kalt et al., 2021; Sun et al., 2022). Energy exhibits disadvantage of an insufficient conversion rate, a high production cost and an unstable capacity; consequently, the main force of power generation remains thermal power. However, thermal power plants generate many pollutants during power generation (Roy et al., 2021). Dey et al (2021) and Nasir et al. (2021) thought that the traditional generation mode is inconsistent with the current social background of energy conservation and environmental protection. To achieve cleaner and sustainable power production, it is necessary to improve the economics of power system dispatch strategies and reduce polluting gas emissions. The aim of economic load dispatch (ELD) is to reasonably allocate the generating power of the units, reduce the operating costs of the power system, improve environmental benefits and obtain cleaner and sustainable electricity.

Nevertheless, the ELD problem is an optimization problem with multiple constraints (Liu et al., 2021). The ELD optimization goal is to reduce generator units’ fuel cost, and the constraints include the generation power constraint, power balance constraint, and prohibited operating areas. The aim of this study is to propose IMRFO-based solution approach to address the energy ELD problem, reduce the fuel cost and increase the resource utilization rate. Deng et al. (2021) and Agrawal et al. (2021) argued that intelligent algorithms with excellent optimization capabilities are not limited by the problem dimension, and are suitable for solving nonlinear and nondifferentiable problems. In the literature, Liu et al. (2021) demonstrated that the complex constraints make the ELD problem become into a nonconvex, discontinuous, multidimensional, and nondifferentiable constraint problem, which increases the solving complexity. Hassan et al. (2021) and Velasquez et al. (2021) argued that there exist two ways to address ELD problems, specifically, by using mathematical optimization methods or intelligent algorithms. The mathematical solution methods, including the gradient method, lambda iteration method, and quadratic programming method, ignore the valve point effect pertaining to the conversion of complex nonconvex cost functions into smooth cost functions.

Moreover, mathematical methods exhibit inferior convergence and easily fall into the local optimal solution. In addition, Deb et al. (2021) and Guo et al. (2021) indicated that mathematical methods involve considerable amounts of calculation as the ELD problem dimension increases. The calculation accuracy is low because mathematical methods use an approximate optimization model to solve the none differentiable problem. Hence, mathematical optimization methods can not address the ELD problem in large power systems, so this study employs the intelligent algorithm-based solution strategy to solve the ELD problem considering different constraints. Many studies have adopted heuristic algorithms, such as particle swarm optimization (Gholamghasemi et al., 2019) and genetic algorithm (Li et al., 2019) to address the ELD problem. However, classical intelligent algorithms have many parameters that need to be adjusted. Agrawal et al. (2021) indicated that randomness of adjustable parameters affected the optimization effect of the algorithms, thereby causing the classic intelligent algorithms less controllable. Hence, variants of heuristic algorithms with superior performance have been devised to solve the ELD problems (Li et al., 2021). In particular, power systems with different scales are applied to prove the effectiveness of the proposed IMRFO-based approach, and the proposed algorithm is compared with state-of-the-art methods.

Manta ray foraging optimization (MRFO) algorithm is widely used in various engineering fields due to its powerful optimization performance (Houssein et al., 2021; Zhao et al., 2020). However, when solving high-dimensional problems, the MRFO algorithm is easy to fall into a local optimal solution, which causes the MRFO algorithm to fail to obtain the optimal solution when solving the ELD problems. Fu et al. (2020) and Deb et al. (2021) believed that the ELD problem includes complex equality and inequality constraints, which belongs to a multi-constrained, high-dimensional and non-convex optimization problem. The ELD problem has higher requirements for the algorithm solving ability. This study proposes an improved manta ray foraging optimization (IMRFO) approach for solving the ELD problems. The adaptive strategy was introduced in the MRFO algorithm and the IMFO algorithm was combined with the differential evolution (DE) algorithm, which improves the effects of the IMRFO-based approach.

The contributions of this study are as follows: (1) The IMRFO algorithm with high optimization ability and convergence speed is proposed; (2) the IMRFO-based method efficiently solves the ELD problem; (3) the IMRFO-based approach reduces the fuel cost of the generator units, which improves the economics of the power system; and (4) cleaner and sustainable power is obtained by improving the economy of power system dispatching strategy. The remaining sections are structured as follows. Section 2 presents the literature review. Section 3 constructs the mathematical model of the ELD. Section 4 introduces the IMRFO. Section 5 describes the verification of the IMRFO-based solution strategy using three ELD-type cases. Section 6 highlights the conclusions and limitations.

2. Literature review

The existing studies for addressing the ELD problems have focused on two ways. The first type of approaches involves mathematical programming methods, such as the lambda iterative method, quadratic programming method, gradient method (D'Angelo and Palmieri, 2021), linear programming method (Li et al., 2021), and Lagrange relaxation method. Shouman et al. (2021) and Dey et al. (2021) argued that mathematical methods involve considerable amounts of calculations due to the constraints of the generator units and increasing scale of power systems when addressing the ELD problem, and the quality of the solutions cannot be guaranteed. For solving complex ELD problems, the mathematical programming methods are difficult to converge to the optimal solution, and it is easy to fall into the local extreme solution, which reduces the applicability of this method. The second type of methods emerged with the advent of intelligent algorithms. Compared with mathematical programming methods, artificial intelligence algorithms have stronger applicability, better solution effects, and are the most widely used. At present, various intelligent algorithms have been developed, such as archimedes optimization algorithm (Hashim et al., 2021), Levy flight distribution algorithm, henry gas solubility optimization algorithm. In addition, intelligent algorithms with different convergence characteristics are applied in different fields. For instance, Houssein et al. (2021) presented an improved Archimedes optimization algorithm to identify PEM fuel cell parameters; Deb et al. (2021) developed turbulent flow of water optimization algorithm to solve ELD problem; and Houssein et al. (2021) used MRFO algorithm for electrocardiogram arrhythmia classification.

Additionally, Lyu et al. (2021) indicated that intelligent algorithms with a high optimization ability are not restricted by the function dimension of the target and are suitable for solving the large-scale ELD problems. Various algorithms have yielded notable results for solving ELD problem, such as PSO (Gaing, 2003), gray wolf optimization algorithms (Anter et al., 2019), and sine and cosine algorithms (Altay and Alatas, 2021). However, intelligent algorithms cannot guarantee the optimization effect when solving the ELD problem under various constraints involving equality and inequality constraints. Hence, verifying the performance of the proposed approaches in addressing the ELD problem with different constraints is necessary.

The first type of ELD problems focuses on the output and input nonlinearities of the generator units. Al-Bahrani et al. (2021) and Zare et al. (2021) highlighted that the valve point effect causes the input and output nonlinearities of the generator units. Notably, Lu et al. (2010) proposed an improved differential evolution-based approach to solve the ELD problem considering the valve point effect. The improved differential evolution (DE) algorithm exhibits superior global search capabilities, and its effectiveness has been proven by applying it to process a problem with 10 power generation units. However, Lu et al. (2010) ignored that the complexity of a 10-unit system is small, therefore, the applicability of the presented algorithm needs to be further studied. In addition, Al-betar et al. (2016) presented a naturally updated harmony search algorithm that considers the output and input nonlinearities of the generator units. Xiong and Shi (2018) proposed a hybrid approach that combines a biogeography-based and brainstorm-based optimization strategy to solve such ELD problems, however, Xiong and Shi (2018) ignored that the hybrid method has complex structure and high computational cost.

The second type of ELD problem focuses on the ramp rate constraint of the generator units and transmission loss of the power system. Fu et al. (2020) argued that such ELD problems place high requirements on the output power change of the generator units; moreover, the transmission loss of the power system obtained by the intelligent algorithms needs to be as low as possible. For instance, Gholamghasemi et al. (2019) proposed an improved PSO-based strategy to solve such ELD problems. The convergence ability of the PSO-based strategy was enhanced using a phasor angle to modify the control parameters of the original algorithm, but Gholamghasemi et al. (2019) ignored that PSO-based strategy cannot effectively get rid of local extremums. In addition, Takeang and Aurasopon (2019) combined the lambda iteration method with a simulated annealing algorithm to present a hybrid strategy for solving ELD. The quality of the solution obtained by the hybrid method is higher, but Takeang and Aurasopon (2019) lacked to analyze the high complexity of the hybrid strategy.

The third type of ELD problem considers equality constraints, inequality constraints and other factors. Li et al. (2019) indicated that such ELD problems bring a higher challenge for the optimization ability of intelligent algorithms as well as their ability to jump out of the local optimal solution. For instance, Pothiya et al. (2008) presented a tabu search-based approach to address the ELD problem. This approach exhibits satisfactory convergence effect when solving different ELD problem types, but ignores the quality of the optimal solution. To improve the quality of solution, Barati and Sadeghi (2018) presented a hybrid approach on the basis of modified PSO and GA to address ELD. The hybrid algorithm achieves enhanced results when applied to small power systems, however, an inferior convergence occurs in the case of medium power systems. In addition, Subathra et al. (2015) presented a novel hybrid approach that combines the sequential quadratic programming (SQP) technology and cross-entropy algorithm (CE). This novel approach effectively addresses complex ELD problems involving equality and inequality constraints, but Subathra et al. (2015) lacked to improve the convergence stability of the hybrid approach. To prevent the DE algorithm from converging prematurely, Niu and Irwin (2014) proposed a DE-based variant through clonal selection, which uses the clonal selection algorithm as a global search method. However, Niu and Irwin (2014) ignored that clonal selection has limited improvement on the quality of solution for ELD.

The energy industry uses various algorithms to address different types of ELD problems. However, the solution effects of the algorithms change due to the various constraints and objective functions considered in the ELD model. To solve different types of ELD problems, this study proposes a novel intelligent algorithm-based solution strategy (Chen et al., 2019; Kalt et al., 2021; Sun et al., 2022). Zhao et al. (2020) proposed the Manta ray foraging optimization algorithm (MRFO) with a simple principle and few control parameters, which is suitable for solving multi-constraint optimization problems. However, the MRFO algorithm involves the limitations of a slow convergence speed and inferior optimization ability. To solve these limits, Hassan et al. (2021) developed a hybrid approach that combined MRFO algorithm with Gradient-based optimizer (GBO). In this approach, GBO algorithm is employed to improve the ability of MRFO algorithm to avoid local extremums. However, Hassan et al. (2021) ignored to balance the local exploitation and global search capabilities of the MRFO algorithm. Therefore, improving the solving ability of MRFO algorithm needs to be further studied. The adaptive strategy has better performance to balance the local exploitation and global search performance of the MRFO algorithm. In addition, the performance of the MRFO algorithm to avoid the local extremes is strengthened using the mutation and crossover strategies of the DE algorithm. Hence, to obtain high quality solutions considering different constraints, the IMRFO-based approach is proposed by incorporating an adaptive strategy, nonlinear convergence factor and DE algorithm. The convergence speed and the ability of avoiding local extremums are enhanced using the abovementioned concepts to ensure that the IMRFO-based strategy obtains the optimal solution for ELD with different constraints. In addition, different scale testing systems are considered to prove the IMRFO-based approach.

3. Economic load dispatch model

ELD solution belongs to a multi-constraint optimization process. The minimum fuel cost of the generator units is identified while meeting the system load requirements and constraints of the generator units. In addition, the operating constraints of the generator units include the equality and inequality constraints.

3.1 Objective function

The defined ELD model is as follows:

$$F_c = \sum_{e=1}^{m} F_e(P_e) = \sum_{e=1}^{m} (\alpha_e P_e^2 + \beta_e P_e + \gamma_e) \tag{1}$$

where F_e is the cost function of the e_{th} generator unit, F_c represents the total fuel cost, m represents the number of generator units, and P_e represents the output power of the e_{th} generator unit. α_e, β_e and Υ_e are the fuel cost coefficients.

The sudden opening and closing of the intake valve results in a valve point effect when the generator unit is operating. This phenomenon makes the cost curves of the generator units nonlinear, so the equation of the objective function is modified as follows:

$$F_c = \sum_{e=1}^{m} F_e(P_e) = \sum_{e=1}^{m} (\alpha_e P_e^2 + \beta_e P_e + \gamma_e + \left|\delta_e \sin(\varepsilon_e (P_{e,\min} - P_e))\right|) \tag{2}$$

where $P_{e,\min}$ is the minimum output power. δ_e and ε_e are the cost coefficients.

Equation (2) indicates that α_e, β_e and Υ_e form a smooth quadratic function. Moreover, δ_e and ε_e form a nonconvex sine function.

3.2 Equation constraint

The power balance constraint is the equality constraint, which ensures that the total output matches the load demand and transmission loss.

$$\sum_{e=1}^{\mathrm{m}} P_e = P_{load} + P_{loss} \tag{3}$$

$$P_L = \sum_{e=1}^{m} \sum_{f=1}^{m} P_e B_1 P_f + \sum_{e=1}^{m} B_2 P_e + B_3 \tag{4}$$

where B_1, B_2 and B_3 are transmission loss coefficients; P_{loss}(MW) indicates the system transmission loss; P_f(MW) is the output of the f_{th} generator unit; and P_{load}(MW) is the load demand.

3.3 Inequality constraints

(1) Generation power constraint

The output of the generator unit must lie between its upper and lower bounds. The generation power constraint is defined as follows:

$$P_{e,\min} \le P_e \le P_{e,\max} \tag{5}$$

where $P_{e,\min}$ and $P_{e,\max}$ represent the lower and upper bounds of the e_{th} generator unit.

(2) Ramp rate limit

Change in the generator output power is limited by the ramp rate constraint, shown in Eq. (6):

$$\max(P_{e,\min}, P_e^0 - DR_e) \le P_e \le \min(P_{e,\max}, P_e^0 + UR_e) \tag{6}$$

where P_e^0 is the output before the change. DR_e and UR_e indicate the ramp-down and ramp-up rate constraints.

(3) Prohibited operation areas

The prohibited operating areas, which are caused by the vibration of the unit bearings or related equipment, is defined as follows:

$$P_j \in \begin{cases} P_e^l \le P_e \le P_{e,1}^L \\ P_{e,j-1}^U \le P_e \le P_{e,j}^L \\ P_{e,NPZ_e}^U \le P_e \le P_e^u \end{cases} \tag{7}$$

where NPZ_e represents the number of prohibited operation areas, $P^L_{e,j}$ (MW) represents the first prohibited operation area, and $P^U_{e,j}$ (MW) represents the maximum (j-1)$_{th}$ prohibited operating area. P^l_e and P^u_e represent the lower and upper output bounds.

4. MRFO and MRFO-based variant

4.1 MRFO

Zhao et al. (2020) imitated the manta ray's foraging behavior in nature to develop the MRFO algorithm that was used to solve the optimization problems in engineering. In addition, Zhao et al. (2020) found that the MRFO algorithm has better solution performance compared with the existing well-known optimization algorithms. Therefore, in this study, MRFO algorithm was employed to solve ELD problem. The MRFO algorithm follows the following principles:

(1) The MRFO is driven by three manta rays' foraging strategies: cyclone foraging, chain foraging and somersault foraging.
(2) The update of each individual is determined by the previous individual and current optimal individual in the chain foraging strategy.
(3) The update of each individual is jointly determined by the previous individual and reference individual in the whirlwind foraging strategy. The reference individual selects the current optimal value or random locations in the search space.
(4) Manta ray individuals perform adaptive search under somersault foraging strategy.

A. Chain foraging

The location of the current individual in chain foraging is described by the previous individual and current optimal individual. The equations of chain foraging are as follows.

$$x_k^d(m+1) = \begin{cases} x_k^d(m) + r \times (x_{best}^d(m) - x_k^d(m)) + a \times (x_{best}^d(m) - x_k^d(m)) \\ x_k^d(m) + r \times (x_{k-1}^d(m) - x_k^d(m)) + a \times (x_{best}^d(m) - x_k^d(m)) \end{cases} \tag{8}$$

$$a = 2 \times r \times \sqrt{|\log(r)|} \tag{9}$$

where $x^d_k(m)$ is the location of the k_{th} individual at time m and dimension d, $x^d_k(m+1)$ is the next position of the k_{th} individual, r is randomly distributed between [0, 1], a is a weight coefficient, and $x^d_{best}(m)$ is the current optimal position.

B. Cyclone foraging

The position of manta rays performing cyclone foraging is updated in two ways. One approach is to implement cyclone foraging operations. The position of a manta ray individual is determined by the positions of the current optimal individual and previous individual. The other approach involves exploring the search space. In this process, the position of a manta ray individual is determined by a random position and the previous individual position. When the manta ray individual performs cyclone foraging, the position equation is expressed as follows:

$$x_k^d(m+1)=\begin{cases} x_{best}^d + r\times(x_{best}^d - x_k^d(m)) + \beta_c \times (x_{best}^d(m) - x_k^d(m)) \\ x_{best}^d + r\times(x_{k-1}^d - x_k^d(m)) + \beta_c \times (x_{best}^d(m) - x_k^d(m)) \end{cases} \tag{10}$$

$$\beta_c = 2e^{r\frac{L-l+1}{L}} \times \sin(2\pi r_1) \tag{11}$$

where β_c is the weight coefficient. L and l denote the maximum and current values of iterations.

When the manta ray individual explores the search space, the mathematical model is formulated as follows:

$$x_{rand}^d = Lb^d + r\times(Ub^d - Lb^d) \tag{12}$$

$$x_k^d(m+1)=\begin{cases} x_{rand}^d + r\times(x_{rand}^d - x_k^d(m)) + \beta_c \times (x_{rand}^d - x_k^d(m)) \\ x_{rand}^d + r\times(x_{k-1}^d - x_k^d(m)) + \beta_c \times (x_{rand}^d - x_k^d(m)) \end{cases} \tag{13}$$

where x^d_{rand} represents the random location; Ub^d and Lb^d represent the upper and lower limits of the d-dimensional search space.

C. Somersault foraging

In somersault foraging, manta ray individuals use the current optimal position as a reference to update their positions, as follows:

$$x_k^d(m+1) = x_k^d(m) + S\times(r_1 \times x_{best}^d - r_2 \times x_k^d(m)) \tag{14}$$

where S(S=2) determines the range of the manta ray's somersault foraging. r_1 and r_2 are random values between [0, 1].

4.2 IMRFO algorithm

A. Adaptive strategy-based somersault foraging

The somersault foraging of the MRFO algorithm is the key during the iterative process, and the optimal value obtained by the MRFO depends largely on the somersault foraging process, but this strategy does not guarantee the ability to balance the globally searching and locally developing of the MRFO algorithm. To better balances the global converging and local searching abilities in the iteration, the sine and cosine adaptive strategies are introduced to the MRFO algorithm. In addition, the search ability of the population deteriorates when the current optimal individual used as a reference falls into the local optimal solution during the somersault process. Through the sine and cosine adaptive strategies, the optimal individual can adaptively update its position in the iterative process, thereby avoiding local extremum solutions.

The improved somersault foraging strategy is defined as follows:

$$x_i^d(t+1) = x_i^d(t) + (C + S + rand) \times (r_2 \times x_{best}^d - r_3 \times x_i^d(t)) \quad (15)$$

$$C = \cos((rand(1) - 0.5) \times \pi) \quad (16)$$

$$S = \sin((rand(1) - 0.5) \times \pi) \quad (17)$$

where t indicates the current value of iterations; C and S are the cosine and sine adaptations. r_3 and r_4 are randomly distributed between [0, 1].

As depicted in equation (15), parameters C and S expand the search range of the manta rays. Through the sine and cosine adaptive strategies, the IMRFO algorithm exhibits a stronger ability of local development and global optimization in the iterative process as well as a better performance to avoid local extremes.

B. Nonlinear convergence factor-based cyclone foraging

A nonlinear convergence factor is introduced in the MRFO cyclone foraging to increase the convergence speed. The equation for the IMRFO cyclone foraging is as follows.

$$x_k^d(m+1) = \begin{cases} w \times (x_{rand}^d + r \times (x_{rand}^d - x_k^d(m)) + \beta_c \times (x_{rand}^d - x_k^d(m))) \\ w \times (x_{rand}^d + r \times (x_{k-1}^d - x_k^d(m)) + \beta_c \times (x_{rand}^d - x_k^d(m))) \end{cases} \quad (18)$$

$$w = w_{\min} + (w_{\max} - w_{\min}) \times \sin(\pi \times \frac{T}{2t} + \pi) + 1 \quad (19)$$

where $w_{\min}$($w_{\min}$=0.2) and $w_{\max}$($w_{\max}$=0.7) are the lower limit and upper limit of the nonlinear convergence factor w.

The nonlinear convergence factor affects the convergence rate of the MRFO algorithm population. The value range of w is set as [0.2, 0.7] according to the existing studies (Li et al., 2021). The convergence ability of the population is dynamically adjusted by changing the value of the convergence factor, thereby accelerating the convergence speed of the algorithm. As indicated in equation (19), w is gradually reduced, which is conducive to the local search. The convergence speed of the IMRFO algorithm in the iterative process is increased by introducing the nonlinear convergence factor, and the locally developing capability is strengthened. The value of the nonlinear convergence coefficient can be adjusted according to the actual problems.

C. Differential Evolutionary Algorithm

Additionally, most individuals in the population will approach the global optimal individual in the iteration, which decreases the diversity of the population. In addition, in the iterative process of the MRFO algorithm, most individuals in the population will approach the global optimal location, which further makes the population diversity worse. The individual positions are disturbed to ensure the diversity and robustness in the iterative process of the IMRFO algorithm by introducing the crossover, mutation, and selection strategies.

A. Mutation

For the e_{th} individual $Z_{e,t}$ at the t_{th} generation, the mutation vector $V_{e,t}$ is used to generate a new individual. The mutation vector is defined as follows:

$$V_{e,t} = D*(Z_{best,t} - Z_{e,t}) + D*(Z_{r1,t} - Z_{r2,t}) \quad (20)$$

$$Z^{*}_{e,t} = V_{e,t} + Z_{e,t} \tag{21}$$

where $Z^{*}_{e,t}$ is a newly created individual. r_1 and r_2 are randomly distributed between the maximum population number and 1. $Z_{best,t}$ is the optimal value at the t_{th} generation. D is the scaling factor, with a value range of [0, 1].

B. Crossover

In the crossover operation, the newly generated variable is binomially crossed with the original variable to expand the population. The crossover operation is expressed as follows:

$$o_{e,k,t} = \begin{cases} Z^{*}_{e,t}, & if\,(rand_e[0,1] \le R) or (k = k_{rand}) \\ Z_{e,t}, & else \end{cases} \tag{22}$$

where R represents the crossover probability, with a value range of [0, 1]. $rand_e$ is randomly distributed between [0, 1].

C. Selection

According to the calculation result of the fitness function, the variable with the highest fitness is selected for retention. The selection operation is expressed as follows:

$$Z_{e,t+1} = \begin{cases} Z^{*}_{e,t}, if \;\; f(Z^{*}_{e,t}) \le f(Z_{e,t}) \\ Z_{e,t}, else \end{cases} \tag{23}$$

where $f(Z^{*}_{e,t})$ and $f(Z_{e,t})$ are fitness functions.

The IMRFO pseudocode is presented in Table 1, and Figure 1 presents the optimization process.

Table 1. IMRFO Pseudo code

Improved Manta ray foraging optimization
Set the population size P, and related parameters.
t=0; Initialize the population and calculate the fitness values.
While (t<I)
For i=1 To P
If rand<0.5 Then // Cyclone foraging
If t/I<rand
The mechanism of manta rays to explore the search space using Eq. (18).
Else
Manta rays for cyclone foraging operation using Eq. (10).
End if
Else // Chain foraging
Manta rays perform chain foraging operation using Eq. (8).
End if
End for
Calculate the fitness values of the current population and update the optimal individual x_{best}.
// Somersault foraging
For i=1 To P
The manta rays perform somersault foraging operation using Eq. (15).
End for

Updated fitness values for manta ray populations.
Perform mutation operation on the obtained optimal value using Eq. (20).
Perform crossover operation on the results obtained by the mutation operation using Eq. (22).
Perform selection operation on the results obtained by the crossover operation using Eq. (23).
Updated fitness values for manta ray populations.
t=t+1
End while
Output the optimal value.

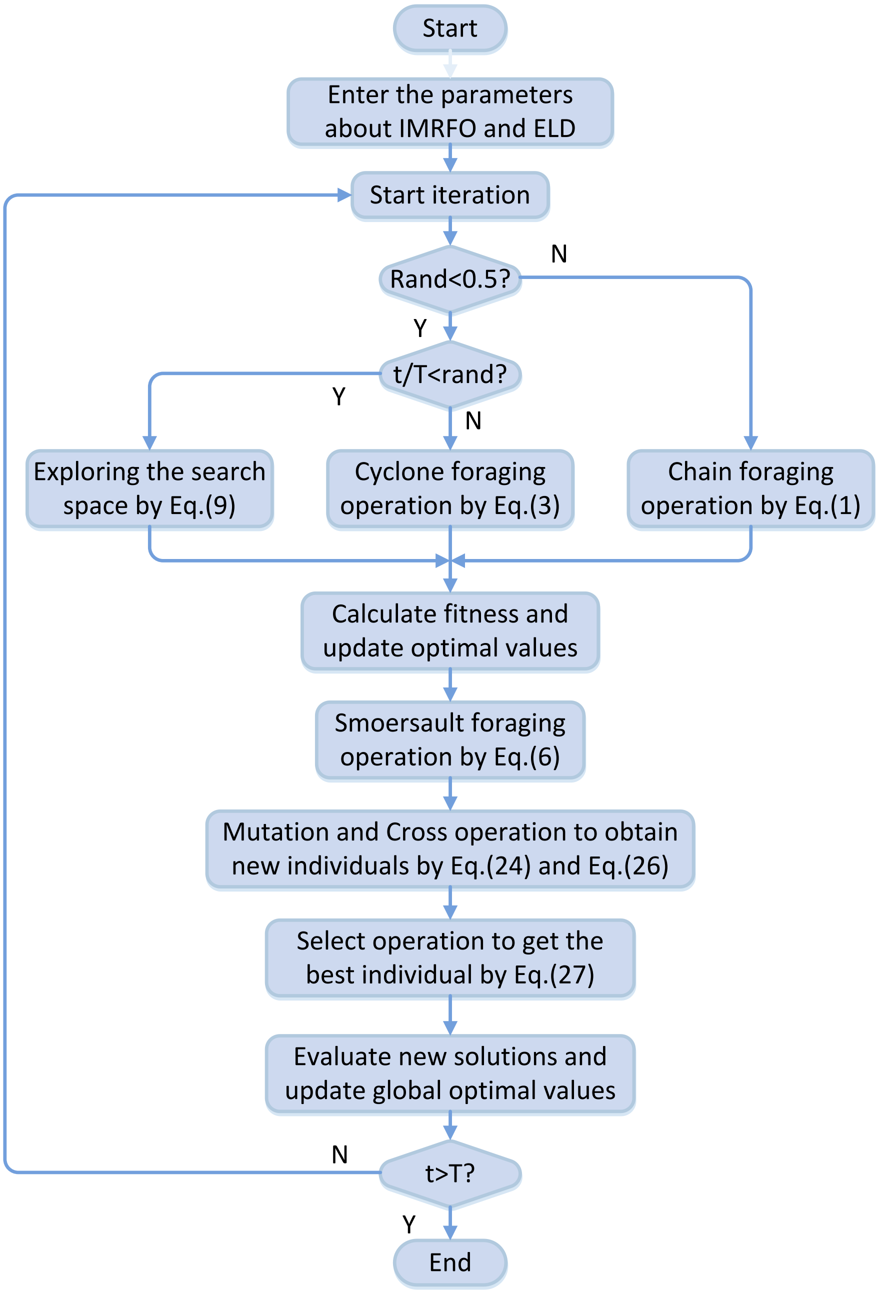

Figure 1. IMRFO optimization process

4.3. Convergence performance verification of the IMRFO

The convergence performance of the IMRFO algorithm was proved employing five benchmark functions. The five benchmark functions are listed in Table 2. Additionally, this study compared the IMRFO technique with the state-of-the-art heuristic algorithms, such as MRFO, PSO, tunicate swarm algorithm (TSA) (Kaur et al., 2020), sailfish optimizer (SFO) (Shadravan et al., 2019) and Harris hawk optimization (HHO) (Heidari et al., 2019). The population numbers and iterations of the six algorithms are set as 30 and 500. To obtain more objective convergence results, each optimization algorithm is implemented 30 times for each benchmark function. The average running time (t_a), minimum value, maximum value, average value and standard deviation (std) obtained by each algorithm in the 30 runs are counted. The statistical results are summarized in Table 3.

Table 2. CEC 2005 benchmark functions

No	Equations	Dimension	Range	Optimum
1	$F_1 = \max_l \{ \lvert k_l \rvert, 1 \le l \le n \}$	30	[-100,100]	0
2	$F_2 = \sum_{l=1}^{n-1} [100 \times (k_{l+1} - k_l^2)^2 + (k_l - 1)^2]$	30	[-10,10]	0
3	$F_3 = \sum_{l=1}^{n} l k_l^4 + random[0,1]$	30	[-1.28,1.28]	0
4	$F_4 = -\sum_{l=1}^{n} (k_l \sin(\sqrt{\lvert k_l \rvert}))$	30	[-500,500]	-12569.48
5	$F_5 = \frac{\pi}{n}(10\sin^2(\pi k_1) + \sum_{l=1}^{30} u(k_l, 10, 100, 4) + K$ $\sum_{l=1}^{n-1} (k_l - 1)^2 (1 + 10\sin^2(\pi k_l + 1)) + (k_n - 1)^2)$	30	[-50,50]	0
6	$F_6 = \sum_{l=1}^{n} k_l^2$	30	[-100, 100]	0
7	$F_7 = \sum_{l=1}^{n} \lvert k_l \rvert + \prod_{l=1}^{n} \lvert k_l \rvert$	30	[-10, 10]	0
8	$F_8 = \sum_{l=1}^{n} [k_l^2 + 10 - 10\cos(2\pi k_l)]$	30	[-5.12, 5.12]	0
9	$F_9 = \frac{1}{4000} \sum_{l=1}^{n} k_l^2 - \prod_{l=1}^{n} \cos(\frac{k_l}{\sqrt{l}}) + 1$	30	[-600, 600]	0

Table 3. Statistics of convergence performance test results

F	Algorithm	Minimum	Maximum	Average	std	t_a /s
F_1	PSO	0.04	0.31	0.16	0.08	0.06
	TSA	1.00E-02	2.29	0.27	0.43	0.12
	MRFO	5.11E-214	1.22E-195	4.08E-197	0	0.16
	SFO	1.77E-08	7.11E-06	1.49E-06	1.54E-06	0.31
	HHO	6.02E-57	8.31E-48	3.00E-49	1.51E-48	0.13
	IMRFO	**0**	**0**	**0**	**0**	0.45
F_2	PSO	18.68	166.97	44.33	34.19	0.06
	TSA	26.34	28.88	28.32	0.81	0.12
	MRFO	15.47	18.69	17.4	0.74	0.17
	SFO	1.90E-03	0.16	3.80E-02	4.08E-02	0.33

	HHO	9.88E-06	9.72E-02	0.01	1.84E-02	0.19
	IMRFO	**1.15E-10**	**0.03E-06**	**6.29E-08**	**1.91E-07**	0.48
F_3	PSO	0.07	0.54	0.23	0.13	0.09
	TSA	3.40E-03	1.72E-02	9.90E-03	3.60E-03	0.17
	MRFO	1.21E-06	2.34E-04	4.16E-05	4.36E-05	0.25
	SFO	2.67E-05	1.70E-03	4.84E-04	4.09E-04	0.41
	HHO	3.73E-06	8.25E-04	1.77E-04	1.77E-04	0.27
	IMRFO	**6.80E-07**	**8.84E-05**	**3.15E-05**	**2.60E-05**	0.60
F_4	PSO	-118.36	-107.14	-115.12	3.22	0.07
	TSA	-4.50E+03	7.11E+03	-6.05E+03	622.20	0.12
	MRFO	-9.88E+03	-7.25E+03	-8.58E+03	648.33	0.16
	SFO	-3.03E+03	-4.62E+03	-3.74E+03	332.21	0.35
	HHO	-1.25E+04	-1.25E+04	-1.25E+04	0.76	0.19
	IMRFO	-1.25E+04	-1.25E+04	-1.25E+03	0	0.47
F_5	PSO	9E-16	0.1	0.01	0.03	0.18
	TSA	1.18	15.33	7.87	3.72	0.29
	MRFO	7.52E-14	4.56E-11	3.38E-11	8.13E-12	0.48
	SFO	1.54E-09	0.21	1.43E-02	4.36E-02	0.62
	HHO	8.19E-09	7.21E-05	8.21E-06	1.59E-05	0.59
	IMRFO	**1.62E-32**	**1.59E-29**	**8.88E-31**	**3.05E-30**	0.98

Continued Table 3. Statistics of convergence performance test results

F	Algorithm	Minimum	Maximum	Average	std	t_a /s
F_6	PSO	493.53	2.82E+03	1.69E+03	633.13	0.05
	TSA	5.46E-24	1.84E-20	1.63E-21	3.48E-21	0.10
	MRFO	**0**	**0**	**0**	**0**	0.15
	SFO	6.73E-14	7.18E-10	8.05E-11	1.75E-10	0.34
	HHO	6.05e-109	1.58e-88	5.27E-90	2.88E-89	0.11
	IMRFO	**0**	**0**	**0**	**0**	0.46
F_7	PSO	15.89	60.52	29.68	9.58	0.06
	TSA	2.81E-15	4.69E-13	9.93E-14	1.12E-13	0.10
	MRFO	1.05E-217	1.83E-206	1.12E-207	0	0.17
	SFO	4.22E-07	1.10E-04	4.01E-05	3.24E-05	0.31
	HHO	1.17E-62	7.59E-49	2.92E-50	1.39E-49	0.11
	IMRFO	**0**	**0**	**0**	**0**	0.43
F_8	PSO	63.98	162.18	116.03	27.32	0.06
	TSA	109.07	329.67	186.71	47.50	0.11
	MRFO	**0**	**0**	**0**	**0**	0.16
	SFO	1.14E-09	3.31E-06	4.08E-07	7.43E-07	0.34
	HHO	**0**	**0**	**0**	**0**	0.17
	IMRFO	**0**	**0**	**0**	**0**	0.42
F_9	PSO	5.51	25.04	16.05	5.58	0.07
	TSA	1.31	13.30	3.19	7.13	0.29
	MRFO	**0**	**0**	**0**	**0**	0.18
	SFO	7.21E-15	9.19E-11	9.66E-12	1.98E-11	0.34
	HHO	**0**	**0**	**0**	**0**	0.19

IMRFO	**0**	**0**	**0**	**0**	0.48

Table 3 showed that the convergence results of the MRFO and IMRFO algorithms were smaller than the results of the PSO and GOA algorithms for the unimodal benchmark function F_1. The maximum value of IMRFO was smaller than that of MRFO. The four statistical indicators of IMRFO were the smallest for the unimodal test functions F_2 and F_3, which proved that IMRFO outperformed the other algorithms in terms of the robustness and optimization ability.

IMRFO converged to the optimal value zero for the multimodal benchmark function F_4, and the standard deviation was zero, which showed the strong global convergence performance of IMRFO. In addition, the IMRFO algorithm obtained the best statistical results for multimodal function F_5. For benchmark functions F_6 to F_9, IMRFO algorithm optimized the global optimal value 0, which further showed strong convergence performance. As for the average running time, PSO algorithm consumed the shortest running time. Additionally, the average running time required by the MRFO and HHO algorithms was similar. The running time of the IMRFO algorithm increased almost doubled compared with the MRFO algorithm. This was because the mutation, crossover, and selection operations in the DE algorithm increase the computational cost to some extent. However, the computing power of current computers has been greatly improved with the development of science and technology, so the increased computing cost will hardly affect computing equipment.

In addition, the IMRFO algorithm was compared with the state-of-the-art variants of meta-heuristic algorithms, such as SDWPSO (Bai et al., 2021), ASSA (Salgotra et al., 2021), and ITSA (Li et al., 2021). Bai et al. (2021) tested the SDWPSO algorithm in 30-dimension. For benchmark functions F_1 to F_3, the average convergence values of SDWPSO algorithm were 5.56E-180, 2.89, and 2.15E-03, and the std values were 0, 3.17E-02, and 1.83E-03. Salgotra et al. (2021) verified the proposed ASSA algorithm using CEC 2005 benchmark functions, and testing demission was 30. For F_6 and F_8, the average value of ASSA algorithm converged to 2.09E-98 and 0. The std values were 8.39E-98 and 0. Generally, the lower the test dimension is, the better the convergence value of the algorithm is and the shorter the running time of the algorithm is. Li et al. (2021) tested the ITSA algorithm in 10-dimension. For benchmark function F_6, the average value of ITSA algorithm converged to 4.81E-229, the average running time was 0.49s. For benchmark function F_7, and the average value of ITSA algorithm converged to 7.40E-127, the std was 3.19E-123, and the average running time was 0.49s. For benchmark function F_8, and the average value of ITSA algorithm converged to 9.51, the std was 5.52, and the average running time was 0.49s. For benchmark function F_9, and the average value of ITSA algorithm converged to 1.67E-12, the std was 1.27E-12, and the average running time was 0.51s. The comparison results revealed that the statistical results of IMRFO were more competitive than the state-of-the-art variants of meta-heuristic algorithms.

The sine cosine adaptive strategies enhance the local search and global exploration performance of IMRFO during the convergence process, and the nonlinear convergence factor increases IMRFO's convergence speed. Moreover, the population diversity of the IMRFO algorithm in the iterative process is maintained through its combination with the differential mutation algorithm, and the algorithm gets rid of the local extremes in the late iteration. Therefore, the improved IMRFO algorithm obtains the most competitive convergence results for unimodal and multimodal test functions.

5. Case studies

Existing studies usually use representative 6-unit (Kaboli and Alqallaf, 2019), 13-unit (Cai et al., 2012; Xu et al., 2019) and 15-unit (Pothiya and Kongprawechnon, 2008; Xu et al., 2019) test systems to verify the effectiveness and advancement of the proposed method. Therefore, in this section, the 6-unit, 13-unit and 15-unit test systems are employed to prove the feasibility of the IMRFO-based solution method, and compares the solution results with the existing methods.

Three ELD case types are used to prove the effectiveness of IMRFO. In each ELD case, the three algorithms run independently 50 times. The maximum, minimum and average values of the fuel cost are considered. In addition, the results obtained by the IMRFO algorithm are compared with those of the PSO and MRFO algorithms. Table 4 lists the parameter settings for IMRFO, MRFO and PSO according to the existing studies.

Table 4. Algorithm parameters

Algorithms	Parameters
IMRFO (Zhao et al., 2020)	P=100, I=1000, F=0.5, R=0.8
MRFO (Zhao et al., 2020)	P=100, I=1000, S=2
PSO (Bai et al., 2021)	P=100, I=1000, A1=1, A2=1.318, w=0.5

Table 4 revealed that the population was set as 100, and the maximum value of iterations for the three algorithms was set as 1000. In IMRFO, the scaling factor F and crossover probability R were set as 0.5 and 0.8. The somersault factor S in the MRFO was 2; in PSO, acceleration factors A1 and A2 were 1 and 1.318. The inertia weight w was 0.5.

5.1 Case1- ELD model considering generator input and output nonlinearities

This case involves a power system, for which the input and output nonlinearities of the generator set are considered. The power system contains 13 generator units. Table 5 lists the test system parameters. The other parameters have been reported by Xu et al. (2019). The total power demand of the power system is 2520 MW. Several state-of-the-art algorithms are considered as comparison methods, such as GA (Cai et al., 2012), CPSO (Cai et al., 2012), GWO (Xu et al., 2019), NGWO (Xu et al., 2019), SA (Victoire and Jeyakumar, 2004), and PSO-SQP (Victoire and Jeyakumar, 2004). Table 6 lists the optimal solution for Case 1.

Table 5. Generator units data of Case 1

Unit	α_e	β_e	γ_e	δ_e	ε_e	$P_{e.\min}$	$P_{e.\max}$
1	2.80e-04	8.10	550.00	300.00	3.50e-02	0.00	680.00
2	5.60e-04	8.10	309.00	200.00	4.20e-02	0.00	360.00
3	3.24e-03	8.10	307.00	200.00	4.20e-02	0.00	360.00
4	3.24e-03	7.74	240.00	150.00	6.30e-02	60.00	180.00
5	3.24e-03	7.74	240.00	150.00	6.30e-02	60.00	180.00
6	3.24e-03	7.74	240.00	150.00	6.30e-02	60.00	180.00
7	3.24e-03	7.74	240.00	150.00	6.30e-02	60.00	180.00
8	3.24e-03	7.74	240.00	150.00	6.30e-02	60.00	180.00
9	3.24e-03	7.74	240.00	150.00	6.30e-02	60.00	180.00
10	2.84e-03	8.60	126.00	100.00	8.40e-02	40.00	120.00

11	2.84e-03	8.60	126.00	100.00	8.40e-02	40.00	120.00
12	2.84e-03	8.60	126.00	100.00	8.40e-02	55.00	120.00
13	2.84e-03	8.60	126.00	100.00	8.40e-02	55.00	120.00

Table 6. The results of different algorithms of Case 1

Unit	FCASO -SQP	GA	PSO -SQP	GWO	CPSO	NGWO	MRFO	IMRFO
1	628.30	627.05	628.32	647.56	628.32	631.00	628.23	628.32
2	299.79	359.40	299.05	306.40	299.83	297.94	299.29	299.20
3	299.19	358.95	298.97	309.61	299.17	299.93	299.31	299.20
4	159.73	158.93	159.47	175.14	159.7	157.93	157.85	159.73
5	159.73	159.73	159.14	66.88	159.64	159.64	159.68	159.73
6	159.73	159.68	159.27	162.75	159.67	159.23	158.88	159.73
7	159.73	159.53	159.54	174.31	159.64	159.76	159.16	159.73
8	159.73	159.89	158.85	61.23	159.65	159.66	158.7	159.73
9	159.73	110.15	159.78	175.14	159.78	159.43	159.62	159.73
10	109.07	77.27	110.96	116.76	112.46	76.88	114.89	77.40
11	77.84	75.00	75.00	116.76	74.00	79.50	77.24	77.40
12	55.00	60.00	60.00	99.92	56.50	86.80	91.87	87.68
13	92.43	55.41	91.64	108.56	91.64	94.19	55.29	92.40
Total Power Generation (MW)	2520.00	2520.00	2520.00	2520.83	2520.00	2520.21	2520.00	2520.00
Optimization error (MW)	0	0	0	0.83	0	0.21	0	0
Fuel Cost (%/h)	24970.91	24418.99	24261.05	24231.18	24211.56	24185.45	24191.82	**24169.91**

Table 6 presents the fuel costs obtained by the different algorithms. The solution result of ELD is related to the convergence performance of the algorithm. The convergence performance of different algorithms is different, and the obtained ELD solution results are also different. Therefore, there is a certain error in the solution results of each algorithm. Table 6 showed that, limited by the solution performance, the scheduling schemes obtained by the GWO and NGWO algorithms deviate from the load demand. The fuel cost obtained by the IMRFO algorithm was the most competitive under the power balance constraint than the state-of-the-art algorithms. The fuel cost obtained by IMRFO was 24169.91 ($/h), which was significantly lower than that obtained using the other algorithms. In Case 1, the IMRFO algorithm exhibits a strong convergence performance and obtains the optimal solution for ELD. Table 7 presents the ratio of the optimal values of PSO, MRFO and IMRFO for Case 1.

Table 7. Ratio of optimal values of PSO, MRFO and IMRFO in Case 1

Load demand (MW)	The Ratios of the optimal Fuel Cost		
	PSO	MRFO	IMRFO
2520	1	0.9942	**0.9933**

The smaller the value of the optimal fuel ratio is, the better the economy of the scheduling method obtained by the algorithm is. The ratio of the optimal fuel cost of the PSO, MRFO and IMRFO algorithms was 1: 0.9942: 0.9933, indicating that the optimal fuel cost obtained by IMRFO was the most competitive. Due to the large scale of the power system, even a small reduction in the fuel cost may bring notable economic benefits for the power system. Table 7 shows that IMRFO more effectively solves ELD problems than PSO and MRFO. Table 8 shows the statistical results in 50 experimental runs.

Table 8. Statistical results of multiple algorithms in Case 1

Algorithm	Fuel cost ($/h)		
	Minimum	Average	Maximum
FCASO-SQP	24190.63	-	-
GA	24418.99	-	-
PSO-SQP	24261.05	-	-
GWO	24231.18	24442.08	32942
CPSO	24211.56	-	-
NGWO	24185.45	24366.12	-
MRFO	24172.04	24335.72	24728.75
IMRFO	**24169.91**	**24330.79**	**24620.09**

In the 50 tests, IMRFO's statistical results were superior to those of MRFO, presenting that the convergence ability of IMRFO was enhanced. The sine and cosine adaptive strategies enhance the adaptive capability of the IMRFO algorithm, which makes the IMRFO algorithm more suitably balance the local mining and global exploration capabilities during the iterative process. The PSO, MRFO and IMRFO convergence curves are shown in Figure 2.

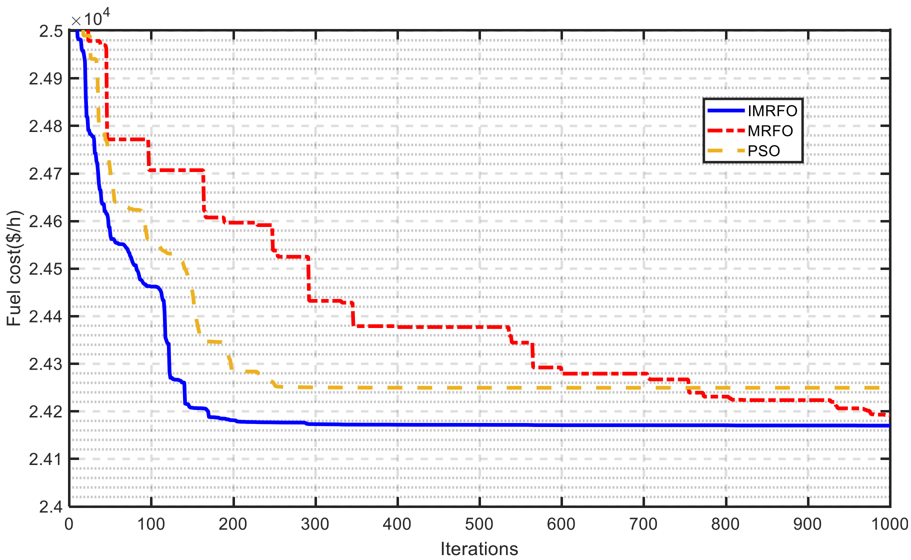

Figure 2. IMRFO, MRFO, and PSO convergence curves in Case 1

Figure 2 revealed that the convergence curve of IMRFO was smoother than that of PSO and MRFO. The convergence curve of MRFO exhibited the lowest convergence speed. The PSO converged after 280 generations; however, the convergence accuracy was low. IMRFO exhibited the highest convergence speed than the MRFO and PSO algorithms, and the iterative curve starts to converge after approximately 230 generations. This phenomenon occurs because the nonlinear convergence factor improves the convergence speed of the IMRFO algorithm, enabling the IMRFO algorithm to promptly converge to the optimal value.

The distribution of the results obtained using IMRFO in 50 experimental runs is shown in Figure 3. The fuel cost obtained by IMRFO fluctuates between 24160.00($/h) and 24700.00($/h). The small fluctuation range highlights that the IMRFO algorithm exhibits a strong robustness. In Case 1, the IMRFO algorithm can obtain a satisfactory solution of the ELD problem.

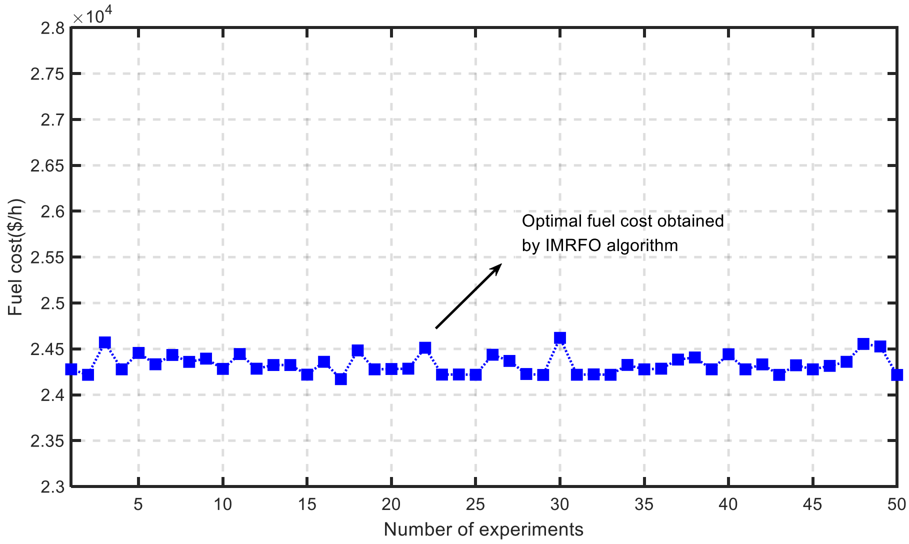

Figure 3. Distribution of results obtained by IMRFO for Case 1

5.2 Case 2- ELD model considering the ramp rate constraint and transmission loss

In Case 2, the ELD model's constraint conditions consider the slope rate constraint and transmission loss in the objective function. Compared with that in Case 1, the constructed ELD model in Case 2 is more complicated and necessitates a higher solving performance of the algorithm. The test system in Case 2 contains six generation sets. Table 9 lists the parameters of the test system, and Table 10 presents the transmission loss matrices of the test system. The parameters of the test system have been detailed in the literature (Kaboli and Alqallaf, 2019). The total power demand of the test system in Case 2 is 1263 MW. In Case 2, GA, PSO (Gaing, 2003), SA (Victoire and Jeyakumar, 2004), GWO, and GWO II (Xu et al., 2019) are used as comparison algorithms.

Table 9. Generator units data of Case 2

Unit	α_e	β_e	γ_e	UR_e	DR_e
1	240.00	7.00	7.00e-03	80.00	120.00
2	200.00	10.00	9.50e-03	50.00	90.00
3	220.00	8.50	9.00e-03	65.00	100.00
4	200.00.	11.00	9.00e-03	50.00	90.00
5	220.00	10.50	8.00e-03	50.00	90.00
6	190.00	12.00	7.50e-03	50.00	90.00

Table 10. Transmission loss matrices of Case 2

B_1	1.70e-03	1.20e-03	7.00e-04	-1.00e-04	-5.00e-04	-2.00e-04
	1.20e-03	1.40e-03	9.00e-04	1.00e-04	-6.00e-04	-1.00e-04
	7.00e-04	9.00e-04	3.10e-03	0.00	-1.00e-03	-6.00e-04
	-1.00e-04	1.00e-04	0.00	2.40e-03	-6.00e-04	-8.00e-04
	-5.00e-04	-6.00e-04	-1.00e-03	-6.00e-04	1.29e-02	-2.00e-04
	-2.00e-04	-1.00e-04	-6.00e-04	-8.00e-04	-2.00e-04	1.50e-03
B_2	-0.39	-0.13	0.70	0.06	0.22	-0.66
B_3	5.60e-03					

Table 11. The results of different algorithms of Case 2

Unit	GA	PSO	SA	GWO	NPSO	GWOⅡ	MRFO	IMRFO
1	474.81	447.50	478.13	446.63	447.47	446.91	449.86	447.79
2	178.64	173.32	163.02	171.77	173.10	172.10	173.51	173.31
3	262.21	263.47	261.71	264.67	262.68	263.89	261.68	263.45
4	134.28	139.06	125.77	141.34	139.42	139.82	139.15	139.05
5	151.90	165.48	153.71	166.54	165.30	164.40	166.20	165.46
6	74.18	87.13	93.80	85.00	87.98	88.82	85.49	87.12
Total Power Generation (MW)	1276.03	1276.01	1276.13	1276.32	1275.96	1276.02	1275.89	1275.88
Loss (MW)	13.02	12.96	13.13	13.31	12.95	13.01	12.96	12.95
Optimization error (MW)	0.01	0.05	0	0.01	0.01	0.01	0.07	0.07
Fuel Cost (%/h)	15459.00	15450.00	15461.10	15450.07	15450.00	15449.96	15449.55	**15,448.98**

For case 2, the optimization error of the SA algorithm is the smallest, but the economy of the scheduling strategy is the worst. The optimization error of the IMRFO algorithm is 0.07MW, and the economy of the resulting dispatch strategy is the most competitive. The fuel cost of IMRFO was 15448.9827($/h) that was smaller than the fuel cost obtained by the state-of-the-art methods.

The ratio of the optimal fuel cost through the PSO, MRFO and IMRFO algorithms is presented in Table 12.

Table 12. Ratio of optimal values of PSO, MRFO and IMRFO in Case 2

Load demand (MW)	The Ratios of the optimal Fuel Cost		
	PSO	MRFO	IMRFO
1263	1	1	0.9990

The rate of optimal fuel cost reflects the economy of the scheduling method obtained by the algorithm, and the smaller the value is, the more significant the effect of reducing the fuel cost of the power system is. Table 12 showed the optimal fuel cost obtained by different algorithms. Although the consideration of the ramp rate constraint and transmission loss increased the difficulty of solving the ELD model, the IMRFO algorithm yielded a satisfactory solution. The optimal fuel cost obtained in Case 2, as indicated in Table 12, clarified that the MRFO and IMRFO algorithms exhibited a superior solving ability for the ELD model considering slope rate constraints and transmission loss, and both algorithms achieved satisfactory solutions. The optimal fuel cost ratios of PSO, MRFO and IMRFO are 1:1:0.9990. The optimal fuel cost obtained by IMRFO was 0.10% smaller than that obtained by PSO. Compared with that obtained using the PSO algorithm, the solution obtained by IMRFO was more economical. The statistical results of each algorithm in 50 experimental runs are presented in Table 13.

Table 13. Statistical results of existing algorithms in Example 2

Algorithms	Fuel cost ($/h)		
	Minimum	Average	Maximum
GA	15524.00	15469.00	15459.00
PSO	15450.00	15454.00	15492.00
SA	15461.00	15488.98	15545.50
GWO	15450.07	15453.41	15487.14
NPSO	15450.00	15452.00	15454.00
GWOⅡ	15449.96	15450.48	15452.41
MRFO	15449.44	15449.48	15449.60
IMRFO	**15448.98**	**15448.98**	**15448.98**

The statistical results of the IMRFO algorithm demonstrated its strong convergence ability and robustness compared with the existing methods. In Case 2, the minimum fuel cost was obtained in 50 runs, which was indicative of strong solution ability. The sine and cosine adaptive strategies render the IMRFO algorithm more likely to get rid of local extreme solution when solving a more complex ELD problem, and thus, the algorithm converges to a higher quality solution.

Figure 4 presented the convergence curves of the PSO, MRFO and IMRFO algorithms. The iterative curve of the IMRFO algorithm declined more rapidly than that of the PSO and MRFO algorithms. The iterative curves of MRFO and PSO converged to the best solution after the 300th and 200th generations. The iterative curves of IMRFO promptly converged to the best solution after the 100th generation and exhibited the highest convergence speed. The IMRFO algorithm considerably enhanced the convergence speed of the MRFO algorithm because the nonlinear convergence factor increased IMRFO's convergence speed of during the iterative process.

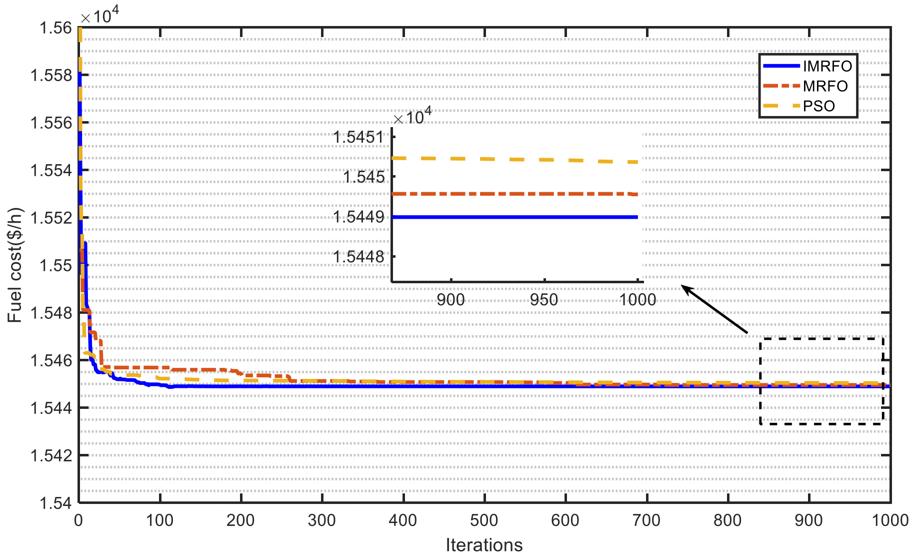

Figure 4. IMRFO, MRFO, and PSO Convergence curves in Case 2

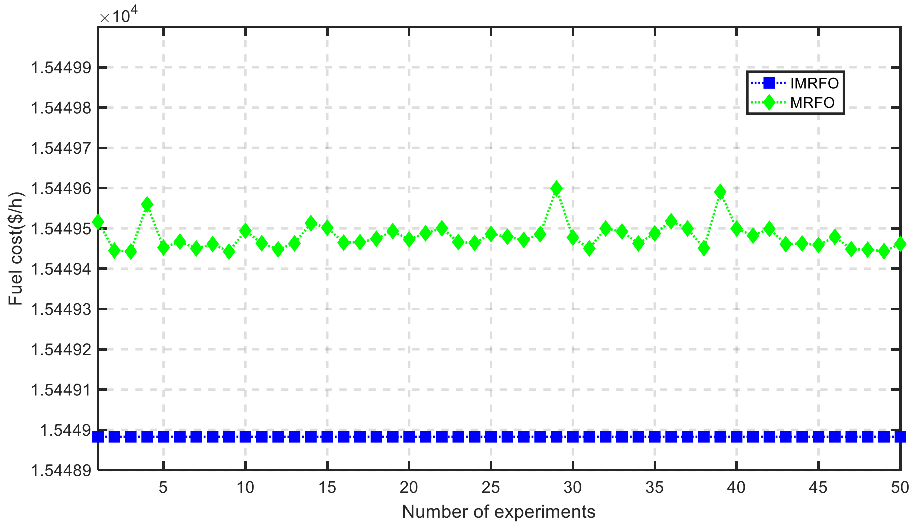

Figure 5. Distribution of results obtained by IMRFO and MRFO in Case 2

The distribution of the fuel cost obtained by the IMRFO and MRFO algorithms in 50 experimental runs is presented in Figure 5. The fluctuation range of the fuel cost obtained using the IMRFO algorithm in 50 runs was small, indicating that the algorithm exhibits a high robustness. The best fuel cost results obtained by the MRFO algorithm in 50 runs showed quite differences, and the fuel cost curve fluctuated considerably, indicating the poor robustness of the algorithm.

5.3 Case 3- ELD model considering the inequality and equality constraints of the generating units

Case 3 involves a medium power system containing 15 generator units. The inequality and equality constraints of the generator unit are considered. Table 14 lists the test system parameters in Case 3 (Xu et al., 2019). The total power demand of the test system is 2630 MW. Compared with those in Cases 1 and 2, the ELD model in Case 3 involves the maximum number of constraints, largest system scale, and highest complexity. Therefore, Case 3 can effectively test the solving performance of the IMRFO-based approach. In addition, the state-of-the-art methods are employed as comparison algorithms, such as GA (Gaing, 2003), PSO (Gaing, 2003), SA (Pothiya and Kongprawechnon, 2008), TS (Pothiya and Kongprawechnon, 2008), NGWO (Xu et al., 2019), and SGA (Kuo, 2008). Table 15 lists the fuel costs obtained by different algorithms.

Table 14. Generator units data of Case 3

Unit	$P^0_{2600.e}$	UR_e	DR_e	$P_{e.\min}$	$P_{e.\max}$	Prohibited Areas
1	400	80	120	150	455	--
2	300	80	120	150	455	[185,255]; [305,355]; [420,450]
3	105	130	130	20	130	--
4	100	130	130	20	130	--
5	90	80	120	150	470	[180,200]; [305,335]; [390,420]
6	400	80	120	135	460	[230,255]; [365,395]; [430,455]
7	350	80	120	135	465	--
8	95	65	100	60	300	--
9	105	60	100	25	162	--
10	110	60	100	25	160	--
11	60	80	80	20	80	--
12	40	80	80	20	80	[30,40]; [55,65]
13	30	80	80	25	85	--
14	20	55	55	15	55	--
15	20	55	55	15	55	--

Table 15. The running results for Case 3

Unit	GA	PSO	SA	TS	NGWO	SGA	MRFO	IMRFO
1	415.31	439.12	453.66	453.54	455.00	455.00	455.00	455.00
2	359.72	407.97	377.61	371.98	380.00	380.00	380.00	380.00
3	104.43	119.63	120.37	129.78	130.00	130.00	130.00	130.00
4	74.99	129.99	126.27	129.34	130.00	130.00	130.00	130.00
5	380.28	151.07	165.3	169.59	160.54	170.00	170.00	170.00
6	426.79	459.99	459.25	457.99	460.00	460.00	460.00	460.00
7	341.32	425.56	422.86	426.89	430.00	430.00	430.00	430.00
8	124.79	98.57	126.40	95.17	84.19	106.25	60.32	60.48
9	133.14	113.49	54.47	76.84	57.78	25.00	69.48	69.43
10	89.26	101.11	149.09	133.5	146.78	160.00	154.04	160.00
11	60.06	33.91	77.96	68.31	80.00	80.00	80.00	80.00
12	50.00	79.96	73.95	79.68	80.00	80.00	80.00	80.00
13	38.77	25.00	25.00	28.31	32.75	25.00	26.79	25.05
14	41.94	41.41	16.06	17.77	17.30	15.00	15.00	15.00
15	22.64	35.61	15.02	22.84	15.48	15.00	18.94	15.02
Total Power Generation	2668.40	2662.40	2663.29	2661.53	2660.54	2661.30	2659.60	2660.04

(MW)								
Ploss (MW)	38.28	32.43	33.27	31.41	30.01	31.26	29.60	30.04
Optimization error (MW)	0.12	0.03	0.02	0.12	0.53	0.04	0	0
Fuel Cost ($/h)	33113.00	32858.00	32786.00	32762.00	32712.00	32711.00	32702.40	**32697.92**

For case 3, the optimization error of the IMRFO algorithm and the MRFO algorithm is the smallest. In addition, the IMRFO algorithm achieved the lowest fuel cost, with a value of 32697.93 ($/h), indicating that the economics of the scheduling strategy obtained by IMRFO are the most competitive. Because the ELD model in Case 3 is more complicated, the algorithms easily fall into local extremes during the solution process, thereby reducing the accuracy of the algorithms. However, even in Case 3, the IMRFO algorithm exhibited a high solution performance and obtained the most competitive solution. This phenomenon occurs because the IMRFO algorithm has stronger local search and global optimization capabilities. Moreover, the mutation strategy ensures the diversity of the IMRFO algorithm and prevents the IMRFO algorithm from falling into a local extremum prematurely, thereby enabling the IMRFO algorithm to yield a superior solution for ELD. Table 16 presents the optimal fuel cost ratios of PSO, MRFO and IMRFO.

Table 16. Ratio of optimal values of PSO, MRFO and IMRFO in Case 3

Load demand (MW)	The Ratios of the optimal Fuel Cost		
	PSO	MRFO	IMRFO
2630	1	0.9952	0.9951

As revealed in Table 16, the optimal fuel cost ratios of PSO, MRFO and IMRFO were 1:0.9952:0.9951, which indicated that the optimal fuel cost calculated by IMRFO was 0.49% smaller than that of PSO. The IMRFO algorithm reduces the fuel cost and enhances the economic benefits for the power system to a certain extent. Compared with cases 1 and 2, the ELD model in case 3 is more complex and more difficult to solve. However, for case 3, the IMRFO algorithm can still obtain the lowest fuel cost, which shows the effectiveness and advancement of the IMRFO algorithm for solving ELD problems. The maximum, minimum and average values of each algorithm in the 50 experiment runs are shown in Table 17.

Table 17. Statistical results of multiple algorithms in Case 3

Method	Fuel cost ($/h)		
	Minimum	Average	Maximum
GA	33113.00	33228.00	33337.00
PSO	32858.00	33039.00	33331.00
SA	32786.00	32869.00	33029.00
TS	32762.00	32822.00	32942.00
NGWO	32830.00	32752.00	32712.00
SGA	32711.00	32802.00	33005.00
MRFO	32698.00	32744.00	32831.00

IMRFO	32697.06	**32697.28**	32700.29

Table 17 presented that although Case 3 was a complex ELD problem involving 15 generator sets, the IMRFO algorithm obtained the optimal solution. The IMRFO algorithm reduced the fuel cost of the generator sets in Case 3 to 32697.28$/h, which was significantly lower than the fuel costs obtained by other approaches, and enhanced the economics of the generator sets. In addition, the maximum, average, and minimum fuel costs obtained by the IMRFO-based approach were similar, indicating that the algorithm exhibits a stable solution performance and high robustness. Case 3 further verified the effectiveness of the IMRFO-based approach for solving complex ELD problems. Figure 6 shows the convergence curves of the PSO, MRFO and IMRFO algorithms.

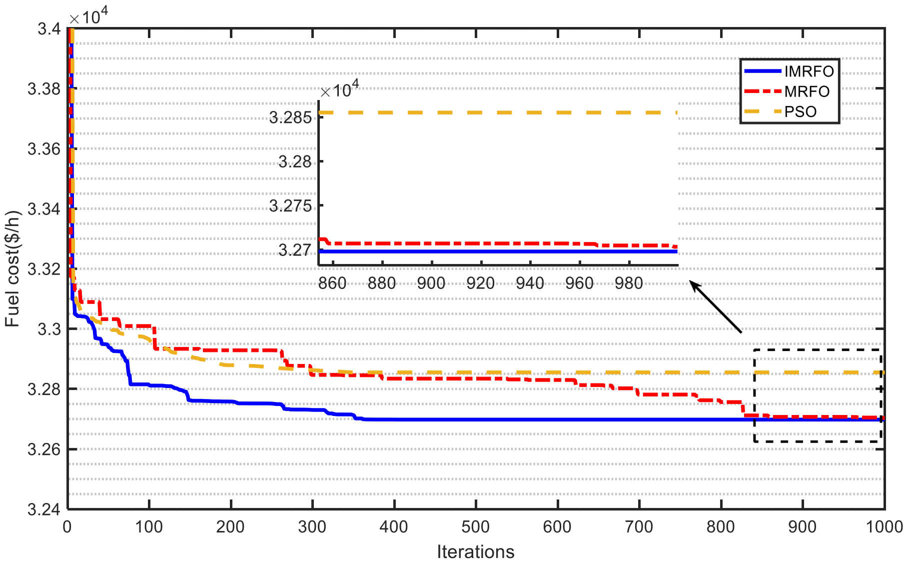

Figure 6. IMRFO, MRFO, and PSO convergence curves in Case 3

The convergence curve of the IMRFO algorithm revealed in Figure 6 was smoother than that of the PSO and MRFO algorithms. The curves of the MRFO, PSO and IMRFO algorithms converged to the optimal value after 850, 400, and 350 generations. The IMRFO algorithm converged to the best solution with a higher speed, however, the MRFO-based approach converged to the best solution in later iterations. The IMRFO algorithm exhibited a higher convergence speed than the MRFO algorithm. For more complex ELD problems, the nonlinear convergence factor and adaptive strategy make the IMRFO algorithm converge to the best solution with a higher speed and exhibit a higher solution accuracy. Figure 7 shows the distribution of the fuel cost obtained by the IMRFO and MRFO algorithms in 50 experimental runs.

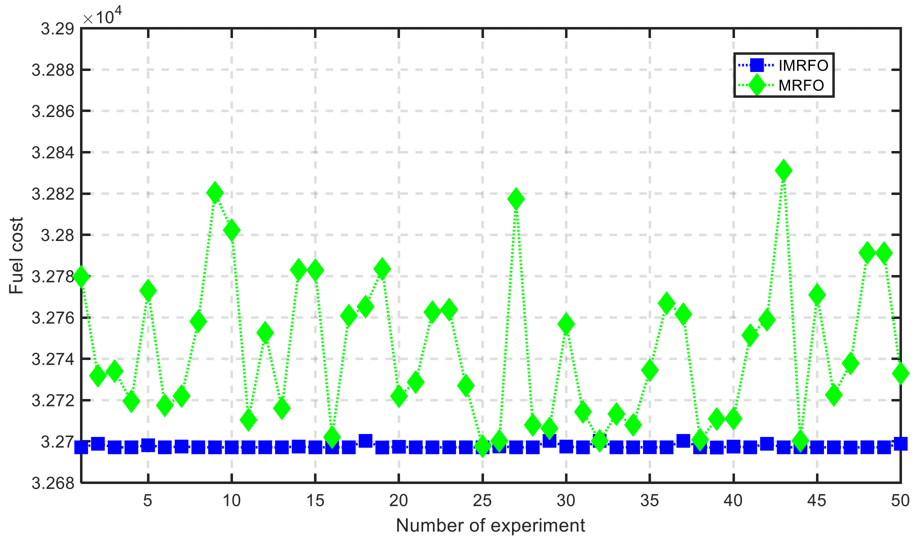

Figure 7. Distribution of results obtained by IMRFO and MRFO in Case 3

Figure 7 revealed that the fuel cost curve obtained by the IMRFO algorithm did not exhibit notable fluctuations, indicating that the IMRFO obtained similar solutions in 50 tests, thereby exhibiting a high solution stability and robustness of the IMRFO algorithm. However, the fuel cost curve obtained using the MRFO algorithm fluctuated sharply, indicating that the solutions obtained by the MRFO algorithm were different in 50 runs, indicating the low solution stability and robustness.

6. Concluding remarks

This study contributes in proposing the IMRFO-based approach for solving the ELD since the ELD model contains complex objective functions and constraints. Intelligent algorithm-based solution strategy has developed into an effective way to solve the ELD problem due to its discontinuous and nondifferentiable nature. However, the high complexity of the ELD problems brings challenges to the intelligent algorithm-based solution strategy, and makes algorithms easily fall into local optimal solutions, thereby reducing the solving effect. In addition, it is necessary to improve the economy of dispatching strategy in order to achieve cleaner and sustainable power production. Hence, this study presents the IMRFO-based approach to solve the ELD problem, and three cases are applied to prove the effectiveness of the proposed approach. The obtained conclusions are as follows:

- IMRFO-based solution approach is proposed for solving the ELD problems with different constraints.
- The economic benefits of the power system are effectively improved by reasonably distributing generator units' output.
- The fuel costs calculated using IMRFO-based strategy are 24169.91($/h), 15448.98($/h) and 32697.92($/h) for the three cases containing 13, 6 and 15 generator units.
- High-quality solutions of the ELD problems efficiently increases the economic benefits of the power system and reduces the energy waste.

The IMRFO-based solution approach contributes in reasonably allocating the generator output, reducing the fuel costs, and enhancing the economic benefits of power systems. However, this study involves the following limitations. First, when the ELD model contains multiple constraints and objective functions, the complexity of the model increases, and the algorithm's solving ability is required to be high. Therefore, the ability of IMRFO algorithm to avoid extreme local value solution needs to be further strengthened to improve the effect of IMRFO algorithm in solving complex ELD problems. Second, the adaptability of the solution algorithm is different for power systems of different scales. If the scalability of the solution algorithm is poor, accurate results cannot be obtained. Hence, the scalability of the proposed solution approach should be further enhanced to adapt to different scale power systems. Third, when constructing the ELD model, the pollutant gas emission objective function is not considered, so the constructed ELD model cannot reflect the environmental protection of the power system. Future research will focus on resolving the above limitations.

Acknowledgements

This study was supported by the key project of Tianjin Natural Science Foundation [Project No. 19JCZDJC32100] and the Natural Science Foundation of Hebei Province of China [Project No. E2018202282].

References

1. Al-Bahrani, L., Seyedmahmoudian, M., Horan, B., Stojcevski, A. (2021). Solving the Real Power Limitations in the Dynamic Economic Dispatch of Large-Scale Thermal Power Units under the Effects of Valve-Point Loading and Ramp-Rate Limitations. Sustainability, 13(3), 26.
2. Al-Betar, M. A., Awadallah, M. A., Khader, A. T., Bolaji, A. L. a., Almomani, A. (2016). Economic load dispatch problems with valve-point loading using natural updated harmony search. Neural Computing and Applications, 29(10), 767-781.
3. Altay, E. V., Alatas, B. (2021). Differential evolution and sine cosine algorithm based novel hybrid multi-objective approaches for numerical association rule mining. Information Sciences, 554, 198-221.
4. Anter, A. M., Wei, Y. C., Su, J. H., Yuan, Y. M., Lei, B. Y., Duan, G. X., Zhang, Z. G. (2019). A robust swarm intelligence-based feature selection model for neuro-fuzzy recognition of mild cognitive impairment from resting-state fMRI. Information Sciences, 503, 670-687.
5. Agrawal, A., Ghune, N., Prakash, S., Ramteke, M. (2021). Evolutionary algorithm hybridized with local search and intelligent seeding for solving multi-objective Euclidian TSP. Expert Systems with Applications, 181, 13.
6. Bai, B., Zhang, J. Y., Wu, X., Zhu, G. W., Li, X. Y. (2021). Reliability prediction-based improved dynamic weight particle swarm optimization and back propagation neural network in engineering systems. Expert Systems with Applications, 177, 13.
7. Barati, H., Sadeghi, M. (2018). An efficient hybrid MPSO-GA algorithm for solving non-smooth/non-convex economic dispatch problem with practical constraints. Ain Shams Engineering Journal, 9(4), 1279-1287.
8. Cai, J., Li, Q., Li, L., Peng, H., Yang, Y. (2012). A hybrid CPSO–SQP method for economic dispatch considering the valve-point effects. Energy Conversion and Management, 53(1), 175-181.
9. Chen, W.C., Chen, W.K., Chen, CW. & Lo, C.C. (2019) An empirical study of willingness to renewable energy installation using importance-performance analysis: the case of Taiwan, Journal of Industrial and Production Engineering, 36(7), 451-460

10. D'Angelo, G., Palmieri, F. (2021). GGA: A modified genetic algorithm with gradient-based local search for solving constrained optimization problems. Information Sciences, 547, 136-162.
11. Deb, S., Abdelminaam, D. S., Said, M., Houssein, E. H. (2021). Recent methodology-based Gradient-Based optimizer for economic load dispatch problem. IEEE Access, 9, 44322-44338.
12. Deb, S., Houssein, E. H., Said, M., Abdelminaam, D. S. (2021). Performance of turbulent flow of water optimization on economic load dispatch problem. IEEE Access, 9, 77882-77893
13. Deng, W., Xu, J. J., Song, Y. J., Zhao, H. M. (2021). Differential evolution algorithm with wavelet basis function and optimal mutation strategy for complex optimization problem. Applied Soft Computing, 100, 16.
14. Dey, B., Bhattacharyya, B., & Marquez, F. P. G. (2021). A hybrid optimization-based approach to solve environment constrained economic dispatch problem on microgrid system. Journal of Cleaner Production, 307, 14.
15. Fu, C., Zhang, S. Q., Chao, K. H. (2020). Energy Management of a Power System for Economic Load Dispatch Using the Artificial Intelligent Algorithm. Electronics, 9(1), 19.
16. Gaing, Z. L. (2003). Particle swarm optimization to solving the economic dispatch considering the generator constraints. IEEE Trans. Power Syst., 18(3), 1187-1195.
17. Gholamghasemi, M., Akbari, E., Asadpoor, M. B., Ghasemi, M. (2019). A new solution to the non-convex economic load dispatch problems using phasor particle swarm optimization. Applied Soft Computing, 79, 111-124.
18. Guo, F. H., Li, G. Q., Wen, C. Y., Wang, L., Meng, Z. Y. (2021). An Accelerated Distributed Gradient-Based Algorithm for Constrained Optimization with Application to Economic Dispatch in a Large-Scale Power System. Ieee Transactions on Systems Man Cybernetics-Systems, 51(4), 2041-2053.
19. Hassan, M. H., Houssein, E. H., Mahdy, M. A., Kamel, S. (2021). An improved Manta ray foraging optimizer for cost-effective emission dispatch problems. Engineering Applications of Artificial Intelligence, 100, 20.
20. Hashim, F. A., Hussain, K., Houssein, E. H., Mabrouk, M. S., Al-Atabany, W. (2021). Archimedes optimization algorithm: a new metaheuristic algorithm for solving optimization problems. Applied Intelligence, 51(3), 1531-1551.
21. Heidari, A. A., Mirjalili, S., Faris, H., Aljarah, I., Mafarja, M., Chen, H. L. (2019). Harris hawks optimization: Algorithm and applications. Future Generation Computer Systems-the International Journal of Escience, 97, 849-872.
22. Houssein, E. H., Ibrahim, I. E., Neggaz, N., Hassaballah, M., Wazery, Y. M. (2021). An efficient ECG arrhythmia classification method based on Manta ray foraging optimization. Expert Systems with Applications, 181, 16.
23. Houssein, E. H., Helmy, B. E. D., Rezk, H., Nassef, A. M. (2021). An enhanced Archimedes optimization algorithm based on Local escaping operator and Orthogonal learning for PEM fuel cell parameter identification. Engineering Applications of Artificial Intelligence, 103, 22.
24. Kalt, G., Thunshirn, P., Wiedenhofer, D., Krausmann, F., Haas, W., Haberl, H. (2021). Material stocks in global electricity infrastructures - An empirical analysis of the power

sector's stock-flow-service nexus. Resources Conservation and Recycling, 173.
25. Kaur, S., Awasthi, L. K., Sangal, A. L., Dhiman, G. (2020). Tunicate Swarm Algorithm: A new bio-inspired based metaheuristic paradigm for global optimization. Engineering Applications of Artificial Intelligence, 90, 29.
26. Kim, J., Kim, K. K. K. (2020). Dynamic programming for scalable just-in-time economic dispatch with non-convex constraints and anytime participation. International Journal of Electrical Power & Energy Systems, 123, 15.
27. Kuo, C.-C. (2008). A novel string structure for economic dispatch problems with practical constraints. Energy Conversion and Management, 49(12), 3571-3577.
28. Li, L. L., Liu, Z. F., Tseng, M. L., Zheng, S. J., Lim, M. K. (2021). Improved tunicate swarm algorithm: Solving the dynamic economic emission dispatch problems. Applied Soft Computing, 108, 14.
29. Li, P., Yang, M., Wu, Q. W. (2021). Confidence interval based distributionally robust real-time economic dispatch approach considering wind power accommodation risk. IEEE Transactions on Sustainable Energy, 12(1), 58-69.
30. Li, Z., Zou, D., Kong, Z. (2019). A harmony search variant and a useful constraint handling method for the dynamic economic emission dispatch problems considering transmission loss. Engineering Applications of Artificial Intelligence, 84, 18-40.
31. Li, L. L., Liu, Z. F., Tseng, M. L., Jantarakolica, K., Lim, M. K. (2021). Using enhanced crow search algorithm optimization-extreme learning machine model to forecast short-term wind power. Expert Systems with Applications, 184.
32. Liu, Z. F., Li, L. L., Liu, Y. W., Liu J. Q., Li, H. Y., Shen, Q. (2021). Dynamic economic emission dispatch considering renewable energy generation: A novel multi-objective optimization approach. Energy, 235.
33. Lu, Y., Zhou, J., Qin, H., Li, Y., Zhang, Y. (2010). An adaptive hybrid differential evolution algorithm for dynamic economic dispatch with valve-point effects. Expert Systems with Applications, 37(7), 4842-4849.
34. Lyu, C., Jia, Y. W., Xu, Z. (2021). A novel communication-less approach to economic dispatch for microgrids. IEEE Transactions on Smart Grid, 12(1), 901-904.
35. Nasir, M., Sadollah, A., Aydilek, I. B., Ara, A. L., Nabavi-Niaki, S. A. (2021). A combination of FA and SRPSO algorithm for combined heat and power economic dispatch. Applied Soft Computing, 102, 35.
36. Niu, Q., Li, K., Irwin, G. W. (2014). Differential evolution combined with clonal selection for dynamic economic dispatch. Journal of Experimental & Theoretical Artificial Intelligence, 27(3), 325-350.
37. Pothiya, S., Ngamroo, I., Kongprawechnon, W. (2008). Application of multiple tabu search algorithm to solve dynamic economic dispatch considering generator constraints. Energy Conversion and Management, 49(4), 506-516.
38. Roy, S., Lam, Y. F., Hung, N. T., Chan, J. C. L., Fu, J. S. (2021). Development of 2015 Vietnam emission inventory for power generation units. Atmospheric Environment, 247, 11.
39. Salgotra, R., Singh, U., Singh, S., Singh, G., Mittal, N. (2021). Self-adaptive salp swarm algorithm for engineering optimization problems. Applied Mathematical Modelling, 89, 188-207.
40. Subathra, M. S. P., Selvan, S. E., Victoire, T. A. A., Christinal, A. H., Amato, U. (2015). A

hybrid with cross-entropy method and sequential quadratic programming to solve economic load dispatch problem. IEEE Systems Journal, 9(3), 1031-1044.

41. Sun W., Zhang, H., Tseng, Ml., Zhang W. & Li X.(2022) Hierarchical energy optimization management of active distribution network with multi-microgrid system, Journal of Industrial and Production Engineering, 39(3), 210-229
42. Shadravan, S., Naji, H. R., Bardsiri, V. K. (2019). The Sailfish Optimizer: A novel nature-inspired metaheuristic algorithm for solving constrained engineering optimization problems. Engineering Applications of Artificial Intelligence, 80, 20-34.
43. Shouman, N., Hegazy, Y. G., Omran, W. A. (2021). Hybrid Mean Variance Mapping Optimization Algorithm for Solving Stochastic Based Dynamic Economic Dispatch Incorporating Wind Power Uncertainty. Electric Power Components and Systems, 48(16-17), 1786-1797
44. Takeang, C., Aurasopon, A. (2019). Multiple of Hybrid Lambda Iteration and Simulated Annealing Algorithm to Solve Economic Dispatch Problem with Ramp Rate Limit and Prohibited Operating Zones. Journal of Electrical Engineering & Technology, 14(1), 111-120.
45. Tsalavoutis, V. A., Vrionis, C. G., Tolis, A. I. (2021). Optimizing a unit commitment problem using an evolutionary algorithm and a plurality of priority lists. Operational Research, 21(1), 1-54.
46. Velasquez, M. A., Quijano, N., Cadena, A. I., Shahidehpour, M. (2021). Distributed stochastic economic dispatch via model predictive control and data-driven scenario generation. International Journal of Electrical Power & Energy Systems, 129, 14.
47. Victoire, T. A. A., Jeyakumar, A. E. (2004). Hybrid PSO–SQP for economic dispatch with valve-point effect. Electric Power Systems Research, 71(1), 51-59.
48. Xiong, G., Shi, D. (2018). Hybrid biogeography-based optimization with brain storm optimization for non-convex dynamic economic dispatch with valve-point effects. Energy, 157, 424-435.
49. Xu, J., Yan, F., Yun, K., Su, L., Li, F., Guan, J. (2019). Noninferior Solution Grey Wolf Optimizer with an Independent Local Search Mechanism for Solving Economic Load Dispatch Problems. Energies, 12(12), 2274.
50. Zare, M., Narimani, M. R., Malekpour, M., Azizipanah-Abarghooee, R., Terzija, V. (2021). Reserve constrained dynamic economic dispatch in multi-area power systems: An improved fireworks algorithm. International Journal of Electrical Power & Energy Systems, 126, 14.
51. Zhao, W. G., Zhang, Z. X., Wang, L. Y. (2020). Manta ray foraging optimization: An effective bio-inspired optimizer for engineering applications. Engineering Applications of Artificial Intelligence, 87, 25.
52.